On Capabilities and Limitations of Current Fast Neutron Flux Monitoring Instrumentation for the Demo LFR ALFRED

Luigi Lepore
SAPIENZA, University of Rome,
SBAI Department, Via Antonio Scarpa,
14-00161 Rome, Italy
e-mail: luigi.lepore@uniroma1.it

Romolo Remetti
SAPIENZA, University of Rome,
SBAI Department, Via Antonio Scarpa,
14-00161 Rome, Italy
e-mail: romolo.remetti@uniroma1.it

Mauro Cappelli
ENEA FSN-FUSPHY-SCM,
Frascati Research Center,
Via Enrico Fermi,
45-00044 Frascati (Rome), Italy
e-mail: mauro.cappelli@enea.it

Among GEN IV projects for future nuclear power plants, lead-cooled fast reactors (LFRs) seem to be a very interesting solution due to their benefits in terms of fuel cycle, coolant safety, and waste management. The novelty of this matter causes some open issues about coolant chemical aspects, structural aspects, monitoring instrumentation, etc. Particularly, hard neutron flux spectra would make traditional neutron instrumentation unfit to all reactor conditions, i.e., source, intermediate, and power range. Identification of new models of nuclear instrumentation specialized for LFR neutron flux monitoring asks for an accurate evaluation of the environment the sensor will work in. In this study, thermal hydraulics and chemical conditions for the LFR core environment will be assumed, as the neutron flux will be studied extensively by the Monte Carlo transport code MCNPX (Monte Carlo N-Particles X-version). The core coolant's high temperature drastically reduces the candidate instrumentation because only some kinds of fission chambers and self-powered neutron detectors can be operated in such an environment. This work aims at evaluating the capabilities of the available instrumentation (usually designed and tailored for sodium-cooled fast reactors) when exposed to the neutron spectrum derived from the Advanced Lead Fast Reactor European Demonstrator, a pool-type LFR project to demonstrate the feasibility of this technology into the European framework. This paper shows that such a class of instrumentation does follow the power evolution, but is not completely suitable to detect the whole range of reactor power, due to excessive burnup, damages, or gamma interferences. Some improvements are possible to increase the signal-to-noise ratio by optimizing each instrument in the range of reactor power, so to get the best solution. The design of some new detectors is proposed here together with a possible approach for prototyping and testing them by a fast reactor. [DOI: 10.1115/1.4033697]

1 Introduction

Nowadays, the fast reactor R&D domain has known important improvements, due mainly to the goals proposed by the GEN IV International Forum [1,2].

Among the proposed solutions, lead-cooled fast reactors (LFRs) have recently gained a position despite the fact that the main drawback about this coolant, i.e., its chemical compatibility with materials, has not yet been solved. Experiments with Pb coolant started in the 1960s in the United States, but they were abandoned soon. In parallel, the Soviet Union developed some land prototypes oriented to conceive a small LFR for marine propulsion. The Soviet Union's experience with lead–bismuth eutectic (LBE, not pure lead) was successful compared with the Americans': the last LFR propelled submarine was dismissed in 1996, after some tens of years of proper duty. However, both countries acknowledged the corrosion processes and chemical compatibility with materials as the main limitation for this technology [3].

Today, R&D in Materials Science makes the lead-coolant attractive once again for critical (power reactor) and subcritical applications [accelerator-driven system (ADS)], due to some advantages with safety, if compared with sodium. As a consequence, in the last decade, lead applications for fast reactors experienced a boost.

Inside the European framework, ongoing LFR projects are the Multi-purpose hYbrid Research Reactor for High-tech Applications (MYRRHA) and Advanced Lead Fast Reactor European Demonstrator (ALFRED), the first being a subcritical demonstrator for an ADS-type plant (whose operability will confirm the possibility to close the uranium fuel cycle by burning all the long-lived actinides), and the second being a medium-power demonstrator reactor for electricity production [4,5]. Currently, MYRRHA is the European pilot plant for the lead technology.

Considering that the sodium-cooled fast reactor (SFR) technology can count on decades of reactor years operation, LFR technology appears today not much investigated as it would deserve.

On the basis of a previous work presented by the authors [6], this paper focuses on I&C issues regarding the demonstrator ALFRED, aiming at showing that the reference neutron instrumentation currently available for SFRs may not be completely suitable when transferred to LFRs. Compared with [7], this work benefits from updated calculations on the ALFRED simulation model, showing new considerations about the applicability of the analyzed instrumentation.

2 Methodology

Choosing the best detector for monitoring a certain physical quantity requires the determination of the environmental conditions to be monitored because some external constraints can limit the sensor functioning or its applicability. Moreover, after the verification of the sensor usability, its performances should be verified as well: Unexpected variation can be produced by external conditions different from a standard/reference point, e.g., a pressure sensor output can be affected by the temperature of the environment in which it is installed.

Neutron flux monitoring instrumentation performances are usually tested in the factory by thermal neutrons while fast response is

Manuscript received October 7, 2015; final manuscript received August 30, 2016; published online October 12, 2016. Assoc. Editor: Leon Cizelj.

never evaluated. This is due to the fact that in a light-water reactor—the most widespread type of reactor in the world—sensors monitor most of all thermal neutrons in every position they are placed, because the variation of sensor positioning significantly affects the magnitude of the neutron flux but does not affect the energy distribution of neutrons.

Fast reactors behave quite differently. The averaged energy of the neutron spectrum significantly varies when moving from the center to the edge of the core. It means that the detector sensitivity varies substantially with positioning because the spectrum-averaged cross-section of the reaction it uses for counting neutrons is no longer constant. In other words, detector performances into a fast reactor environment are practically unknown because different neutron energy spectra lead to detecting capability strongly related to the positioning.

The selection of the correct LFR instrumentation for neutron flux monitoring requires: (1) the identification of sensors robust enough to resist the reactor core thermal-hydraulic conditions, (2) the "actualization" of their performances to the particular LFR neutron environment, and (3) the evaluation of external constraints that may reduce the counter applicability or lifetime.

The so-called actualization has been here realized by the Monte Carlo transport code MCNPX [8], with the mathematical procedure shown below.

A neutron detector response, R (count per second or current), is proportional to the cross-section of the involved reaction i weighted by the energy spectrum of neutrons that hit the sensor (1). The more the cross-section varies with the energy, the more the detector sensitivity can change significantly with the spectrum variation. Referring to Eq. (1), the local value $\bar{\sigma}_i(\rightarrow r)$ provides information about detector sensitivity in position $\rightarrow r$, while its multiplication by local flux $\varphi(E, \rightarrow r)$ gives the local response $R(\rightarrow r)$ of the instrument

$$R(\rightarrow r)\alpha \int \sigma_i(E)\varphi(E, \rightarrow r)\mathrm{d}E = \bar{\sigma}_i(\rightarrow r) \int \varphi(E, \rightarrow r)\mathrm{d}E \quad (1)$$

$$R_{\text{fast}}(\rightarrow r)\alpha\bar{\sigma}_i(\rightarrow r)|_{\text{fast}} \int p(\rightarrow r)\psi(E)|_{\text{fast}}\mathrm{d}E$$

$$R_{\text{thermal}}(\rightarrow r)\alpha\bar{\sigma}_i(\rightarrow r)|_{\text{thermal}} \int p(\rightarrow r)\psi(E)|_{\text{thermal}}\mathrm{d}E \quad (2)$$

$$\text{ESCF}(\rightarrow r) = \frac{\bar{\sigma}_i(\rightarrow r)|_{\text{fast}}}{\bar{\sigma}_i(\rightarrow r)|_{\text{thermal}}} \equiv \frac{\bar{\sigma}_i(\rightarrow r)|_{\text{fast}}}{\bar{\sigma}_i|_{\text{thermal}}} \quad (3)$$

$$S(\rightarrow r)|_{\text{fast}} = \text{ESCF}(\rightarrow r) \cdot S|_{\text{thermal}} \quad (4)$$

MCNPX, with its proper utilities called "tallies," can calculate $\bar{\sigma}_i(\rightarrow r)$ values in (1) with no difficulties. Varying the shape factor $\psi(E)$ of the neutron flux $\varphi(E, \rightarrow r) = p(\rightarrow r)\psi(E)$, e.g., once with fast neutron flux, once with thermal neutron flux, it is possible to calculate the theoretical fast and thermal responses, respectively.

Focusing on energy-averaged cross-sections $\bar{\sigma}_i(\rightarrow r)|_{\text{fast}}$ and $\bar{\sigma}_i(\rightarrow r)|_{\text{thermal}}$, it is possible to calculate the energy spectrum correction factor $\text{ESCF}(\rightarrow r)$ (3), which is useful for actualizing the performances given by the technical specifications of the detector (rated by thermal neutrons) to the current application. Because $\bar{\sigma}_i(\rightarrow r)|_{\text{thermal}}$ refers to the factory instrument testing with thermal neutron, it does not depend on reactor position $\rightarrow r$; therefore, we can indicate it as $\bar{\sigma}_i|_{\text{thermal}}$. This value has been calculated with a single MCNPX run with the Maxwell–Boltzmann neutron energy spectrum corresponding to $T = 293$ K.

For the fast neutron spectra, multiple calculations of $\bar{\sigma}_i(\rightarrow r)|_{\text{fast}}$ have been conducted for each reactor position suitable for installing the detector. So, a set of $\text{ESCF}(\rightarrow r)$ corrections has been evaluated, a single value for each studied location (3). Then, the fast sensitivity of the instrument has been updated, retrieving $S(\rightarrow r)|_{\text{fast}}$ values related to reactor position $\rightarrow r$ (4).

Section 5 shows the results of the methodology applied to ALFRED.

Once the correct sensitivity has been calculated, the process of instrumentation selection for a certain position needs to evaluate other parameters, such as the usable lifetime of the detector or the interferences it may experience.

First of all, lifetime can be calculated as the acceptable "aging" of the sensitive volume of the counter, i.e., when a certain maximum burnup value has been achieved. It must be noted, however, that this duration could be theoretical because other constraints may shorten the detector lifetime, e.g., the achievement of the gamma dose limit as advised by the manufacturer.

According to the analyzed detector, the causes that may limit the detector workability should be evaluated by the operator. With a deep knowledge of the matter, he selects the constraints that the counter has not to overcome; then, he can foresee the effective instrument's lifetime.

To make the selection process successful, it is strongly recommended to match the theoretical considerations with the experimental tests, step by step. It is not infrequent that the real tests lead to the discovery of unconsidered aspects that may cause unexpected variations from the expected results.

3 Reference LFR and Simulation Model

The LFR demonstrator called ALFRED has been proposed in the context of the LEADER Project (Lead-cooled European Advanced DEmonstration Reactor, 2010–2013). Its goal is to demonstrate the feasibility of LFR power reactors and to acquire experience for future larger plants like the European Lead Fast Reactor Project.

ALFRED is a 300 MW_{th} pool-type fast reactor cooled by pure lead, fueled with uranium and plutonium mixed oxides, and operating at core temperatures of 400–480°C in–out with 550°C the hottest cladding temperature.

The core is composed of 171 fuel assemblies with two fuel zones, 12 control rods (CRs), 4 safety rods (SRs), and 108 reflector elements in the dummy belt.

The CRs' shutdown system is based on the buoyancy effect with rods inserting from the bottom of the core; SRs' shutdown system's rods pneumatically penetrate the core from the top.

The secondary circuit operates with water/superheated steam at $18\text{E} + 6$ Pa, removing heat from the reactor pool by eight bayonet tube steam generators (SGs) immersed into the lead coolant. Two independent totally passive decay heat removal systems connect directly to the eight principal SGs to remove residual decay heat after the loss of the primary heat removal by the secondary circuit. A vertical cross-section of ALFRED is presented in Fig. 1.

All structures are conceived for being easily disassembled, speeding up inspections and maintenance.

Lead aggressiveness and erosion phenomena are dominated by fine controlling of coolant chemistry and flow velocity. The best materials to be employed seem to be austenitic low-carbon steels (e.g., AISI 316 L), ferritic–martensitic steels (e.g., T91), and titanium steels. Moreover, protective coatings can be applied to those materials, increasing their robustness. Because of lead's high melting point (327.4°C), the coolant "cold" temperature must be at least 400°C to prevent local freezing. Coolant is not pressurized because the core voiding risk is very low (the partial pressure at 400°C is $2.8\text{E} - 5$ Pa while boiling point at $0.1\text{E} + 6$ Pa is 1745°C); only a few bars of inert gas are foreseen (to reduce the contact with the air, and keep the oxygen concentration in coolant: such a control limits the corrosion processes).

More constructive details about ALFRED can be found in Ref. [9].

To reproduce neutron and gamma radiation fields in the position the neutron flux instrumentation is foreseen to be employed, ALFRED has been reproduced into the Monte Carlo code MCNPX in a very detailed way, as to get significant values in terms of spectra and magnitudes of both neutron and gamma fluxes. The simulation

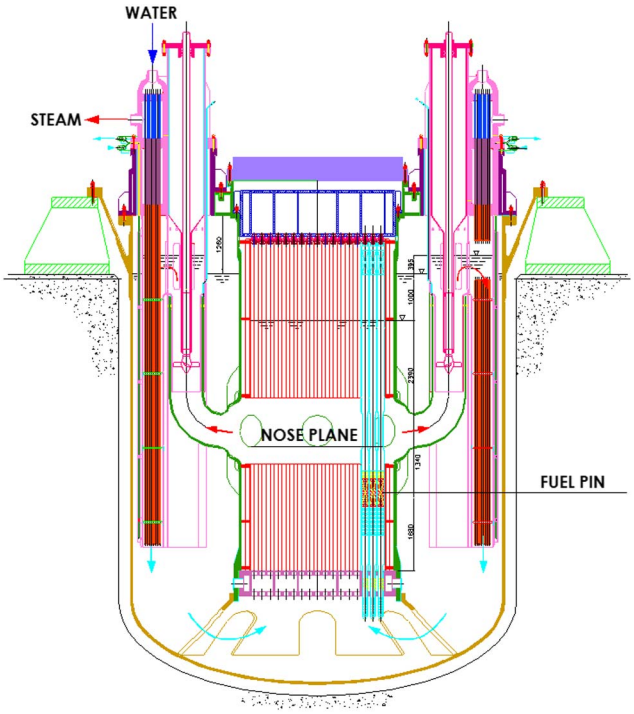

Fig. 1 ALFRED vertical cross-section [9]

model is very complex: Currently, the MCNPX input deck of the reactor reaches 50,000 lines in length, including all the structure surrounding the core. For easiness of running the code, the reactor pit cover has not been included as the main pumps immersed into the lead coolant because those elements are quite far from the core itself and their influences on neutron fluxes near the core may be neglected.

High parallel computing (HPC) resources have been involved, giving the authors the possibility to improve their previous results. Calculations required running time of a single simulation in the order of 300,000 h × core to get the accuracies as desired.

4 Available Neutron Instrumentation for High-Temperature Environment

Small size cores (like ALFRED), usually use out-of-core neutron detectors as control instrumentation because cores result strongly coupled. In nuclear reactor kinetics, it means that a local perturbation propagates all around; then a local effect has global consequences. Paraphrasing to reactor control, in-core perturbation can be easily revealed from out-of-core measurements. In-core monitoring may be useful for providing data about power (and flux) spatial distribution, as to optimize the fuel cycle.

This work focuses on both categories: some miniaturized sensors designed for being installed into fuel-pin lattice are analyzed along with normal-sized detectors for dedicated installation all around the core. Only prompt detectors are taken into account, while instrumentation usable for spatial flux shape analysis only has been evaluated but not analyzed in detector response study in Section 5.

The main drawback for instrumentation to be put into a fast reactor environment is the temperature. Applicable technologies for measuring the neutron flux are limited to some kinds of fission chambers (FCs), and self-powered neutron detectors (SPNDs).

A FC behaves as an electrical condenser: an electrode (usually the cathode) is coated with a thin layer of fissile deposit; when neutrons induce fission events, one of the fission fragments enters the inert gas causing multiple ionization events. It is the starting point of the whole charge creation process. The electron collection to the anode originates a measurable electric signal.

Table 1 Reference data of the currently available FCs [13,14] suitable for Demonstrator ALFRED

		Thermal neutron sensitivity				
Supplier	Product code	Pulse [cps/nv]	MSV [A^2Hz^{-1}/nv]	Current [A/nv]	Diameter [mm]	Length [mm]
Photonis	CFUC06	1	4×10^{-26}	2×10^{-13}	48	412
Photonis	CFUE32	0.001	4×10^{-29}	1×10^{-16}	7	150
Photonis	CFUE43	-	3×10^{-31}	7×10^{-17}	7	85.5

SPNDs must be divided into two categories: beta-decay-based SPNDs and prompt gamma-based SPNDs. For the first category, the absorbed neutron produces a nuclide that emits an electron while decaying; this electron has energy enough to overcome the insulating material between the emitter and the collector electrode: The collection of the beta particles produces the voltage pulse. It is clear that magnitude and collection time of the measurable signal are strongly related to the decay constant of the nuclide used. Beta-decay-based SPNDs give only delayed responses. Vanadium and rhodium SPNDs belong to this family.

Gamma-based SPNDs use prompt gamma ray de-excitation after the neutron capture by a certain atom. The gamma ray (practically concomitant with the capture event) may interact with insulator and collector materials by photoelectric effect, Compton effect, and pair production events, producing collectable electrons. Cobalt and Hafnium SPNDs belong to this category. The fast response time of the electric signal makes such detectors suitable for controlling purposes.

FCs must be supplied with a few hundred volts, whereas SPNDs do not need the supply voltage, making power and signal drivelines in-and-out of the reactor vessel quite simple in comparison with detectors that need some thousands of volts to work (e.g., BF_3 or boron-lined proportional counters).

To improve chemical robustness against the coolant, detectors could be coated with a protective layer for direct installing into lead. However, the best solution seems to be the use of instrumentation guide tubes to protect detectors from direct contact with the coolant, making the handling/replacing/substitution easier as well as their disposal at the end of life. The inert gas pressurization of lead is not important for the selection of detectors. Tables 1 and 2 report the neutron instrumentation currently available for SFR, which could suit the monitoring needs for ALFRED.

Nuclear reactor neutron flux monitoring instrumentation is usually operated in three different modes, namely *pulse* mode, *mean square voltage* (MSV) mode, and *current* mode.

The pulse mode can be used with flux magnitudes up to $1E+6$ n/(cm^2s), which corresponds often to zero-power condition (or source range). This limit was calculated on the hypothesis that the detector sensitivity is 1 cps/nv (taking into account that such a low-neutron radiation field needs a detector sensitivity as high as possible), and the sensor signal pulse width is significantly smaller than 1 μs. Less sensitive instruments, e.g., 0.01 cps/nv, could tolerate pulse mode till $1E+8$ n/(cm^2s), but they could be too "blind" for reactor safe monitoring and start-up. The neutron counting needs to cut the pulses caused by background gammas; therefore, detectors using high Q-value reactions for sensing neutrons are preferred.

With neutron flux from $1E+6$ n/(cm^2s) to $1E+12$ n/(cm^2s), the power is into the intermediate range and MSV mode is operated: the discrimination of gammas background is based on quite different charge releasing and pulse height between electric signals produced by gammas and neutrons. SPNDs, however, cannot be used in such a way.

From $1E+12$ n/(cm^2s) up to $1E+16$ n/(cm^2s), which is the reactor power range, the current mode is applied: the detector

Table 2 Reference data of the currently available SPNDs [18,19] suitable for demonstrator ALFRED

Supplier	Product code	Thermal neutron sensitivity Current [A/nv]	Emitter dimensions [mm]	Overall dimensions [mm]	Thermal burnup [%/month/nv]
KWD Instruments	5503-V-100	5.1×10^{-21}	$D = 2$; $L = 100$	$D = 3.5$	1.2×10^{-15}
KWD Instruments	5503-Rh-50	8.7×10^{-21}	$D = 0.7$; $L = 50$	$D = 2.5$	3.9×10^{-14}
KWD Instruments	5503-Co-210	5.4×10^{-21}	$D = 2$; $L = 210$	$D = 3.7$	1.0×10^{-14}
ARi Industries	V-type	1.54×10^{-21}	$D = 0.5$; $L = 200$	$D = 1.5$	1.3×10^{-15}
ARi Industries	Rh-type	2.4×10^{-20}	$D = 0.5$; $L = 200$	$D = 1.5$	2.3×10^{-14}
ARi Industries	Co-type	3.2×10^{-22}	$D = 0.5$; $L = 200$	$D = 1.5$	1.0×10^{-14}

behaves as a current-mode ion chamber, where a current constant signal is retrieved (this method works only when the gamma background is negligible because gammas cannot be discriminated by neutrons).

In ALFRED, the installation of detectors in proximity of the core causes the neutron flux to be so high that detectors must be operated directly in MSV (if possible) and current modes, according to the power level. As a consequence, the study in Section 5 will show sensitivity and detector response concerning such modes.

5 Application of the Methodology to ALFRED

The methodology described in Section 2 has been applied to the ALFRED reactor, evaluating the capability of the selected instrumentation for neutron flux monitoring.

The study [7] has shown that power monitoring requires most of all MSV and current modes for detector operation. Instrumentation sensitivity and response have been actualized and updated to some reactor positions suitable for installing detectors.

In previous works, two reference planes were considered, and called "core mid-plane" and "nose plane," each one provided with six tally points for energy-averaged cross-section and neutron flux calculation (Fig. 2, left). In this work, new installation points are being considered with a less-invasive approach into the fuel, without failing the neutron core monitoring needs. Two axial segments are being considered (the core central pin—C points—and a reflector pin facing the active zone—R points), leaving the radial segment only on nose plane—N points (Fig. 2, right). The detectors' new positioning has been inspired by the experience acquired with Super-Phénix reactors [10–12].

In these positions, neutron and gamma fluxes have been calculated. Results are shown in Table 3. About neutrons, a more detailed representation of neutron spectra in N1-N4 positions is given in Fig. 4.

As can be easily foreseen, the magnitude of the neutron flux reaches the higher values near the fuel active zone, points C1–C4 and R1–R4. Installation sites farther away, such as points N1–N4 on the nose plane, experience the loss of an order of magnitude in neutron flux if compared with previous points (Fig. 3).

About the neutron energy distribution, for brevity, only some spectra will be presented, e.g., the comparison between the points N1, N2, N3, N4 on the nose plane (Fig. 4), whose variations are easier to understand at a glance. Indeed, spectra vary significantly moving from one position to another, due to the distribution of materials that cause absorption and scattering of neutrons.

As stated in previous works, the sensitivity of the instrumentation may vary significantly (to two orders of magnitude) according to the neutron spectra and peculiar shapes of the reaction cross-sections corresponding to the sensitive materials of the counters.

Among the instrumentation listed in Tables 1 and 2, only the Photonis CFUE32 FC and KWD SPND 5503-Co-210 results will be presented here. Figs. 5 and 6 show significant variations in detector fast sensitivity $S(\rightarrow r)|_{\text{fast}}$ with position $\rightarrow r$: Each detector experiences improvements in sensitivity for out-of-core installation due to the reduction of the averaged energy of neutron spectra and cross-section shapes that generally increase when energy reduces.

Unfortunately, moving from the center of the core through the edges, the flux magnitude $p(\rightarrow r)$ decreases more strongly than those sensitivity gains; therefore, detector responses globally reduce moving away from the core center.

Figs. 7 and 8 show the detector responses in the current mode, $R(\rightarrow r)$, versus different positioning and three different reactor power levels at 0.1%, 10%, and 100% of the nominal thermal power. Even if signals are proportional, schematics of responses at different power levels can help the operator in detectors' selection by comparison with constraints on response values.

About the Photonis CFUE32 FC, it must be noted that the combination among pulse, MSV, and current modes makes the detector operative—theoretically—from zero to the maximum power. Electrical signals are strong enough to be considered as reliable. Because of the high sensitivity, the counter is able to monitor a very low neutron population but also suffers an excessive burnup when power rises. If operated at nominal power, the counter could last only a few months, as stated in previous works [7].

Thanks to the updated calculations in this work, new constraints about workability of the instrument showed up: (1) the

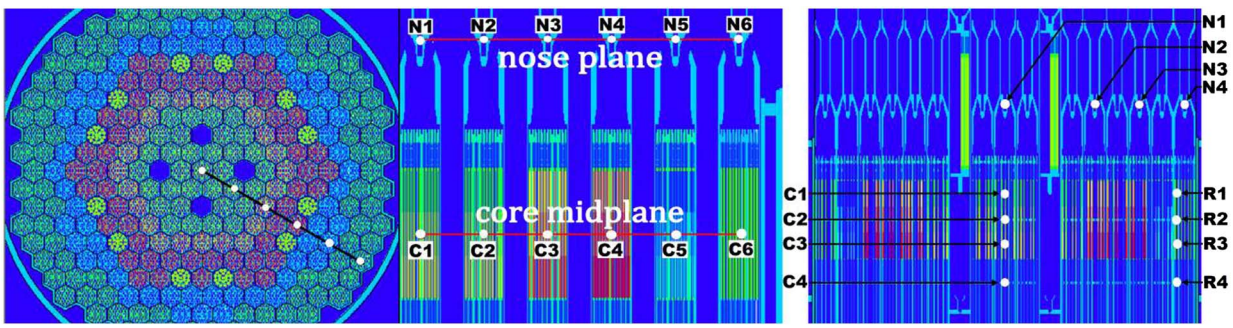

Fig. 2 Core plane and points investigated for calculating detectors' fast sensitivities and responses in previous works (left). New detector's positioning for calculation in this work (right)

Table 3 Neutron and gamma fluxes specification in positions suitable for installing neutron detectors

	Neutron flux [n/(cm^{2}s)] @ 300 MW$_{th}$	Averaged energy [keV]	Thermal (<0.2 eV)	Epithermal (>0.2 eV, <0.1 keV)	Fast (>0.1 keV)
N1	2.47E + 14 (±1%)	26	0.08%	18.91%	81.01%
N2	1.47E + 15 (±1%)	50	0.02%	14.35%	85.62%
N3	2.88E + 14 (±1%)	16	0.21%	28.50%	71.29%
N4	1.33E + 14 (±2%)	13	0.26%	32.60%	67.15%
C1	3.10E + 15 (±0.3%)	150	0.00%	0.90%	99.10%
C2	3.71E + 15 (±0.3%)	150	0.00%	0.73%	99.27%
C3	3.21E + 15 (±0.4%)	150	0.00%	0.93%	99.07%
C4	2.88E + 14 (±1%)	16	0.21%	28.50%	71.29%
R1	7.00E + 14 (±0.8%)	70	0.01%	5.35%	94.64%
R2	7.55E + 14 (±1%)	120	0.00%	5.06%	94.93%
R3	6.15E + 14 (±1%)	120	0.01%	5.43%	94.56%
R4	2.73E + 14 (±0.8%)	33	0.10%	18.53%	81.38%

	Neutron flux [n/(cm^{2}s)] @ 300 MW$_{th}$	Gamma flux [γ/(cm^{2}s)] @ 300 MW$_{th}$	Averaged γ energy [keV]	Air kerma free-in-air rate [Gy/s] @ 300 MW$_{th}$	γ/n flux rates
N1	2.47E + 14 (±1%)	1.65E + 12 (±18%)	950	5.5(±13%)	0.0067
N2	1.47E + 15 (±1%)	1.38E + 12 (±9%)	1450	14(±18%)	0.0009
N3	2.88E + 14 (±1%)	1.29E + 12 (±15%)	1250	8.3(±14%)	0.0039
N4	1.33E + 14 (±2%)	3.62E + 12 (±12%)	900	26.4(±22%)	0.0272
C1	3.10E + 15 (±0.3%)	4.23E + 14 (±2%)	500	1457(±6%)	0.1365
C2	3.71E + 15 (±0.3%)	5.40E + 14 (±2%)	450	1767(±6%)	0.1456
C3	3.21E + 15 (±0.4%)	4.70E + 14 (±4%)	500	1536(±7%)	0.1464
C4	2.88E + 14 (±1%)	1.64E + 13 (±4%)	900	93(±6%)	0.0569
R1	7.00E + 14 (±0.8%)	1.39E + 14 (±8%)	500	438(±12%)	0.1986
R2	7.55E + 14 (±1%)	1.42E + 14 (±5%)	600	566(±16%)	0.1881
R3	6.15E + 14 (±1%)	1.59E + 14 (±18%)	450	472(±13%)	0.2585
R4	2.73E + 14 (±0.8%)	4.21E + 12 (±8%)	900	22.2(±12%)	0.0154

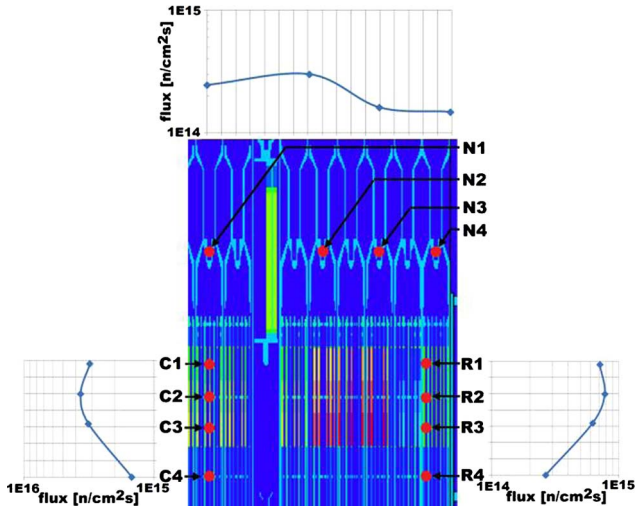

Fig. 3 Neutron flux magnitude trend in positions suitable for installing neutron detectors

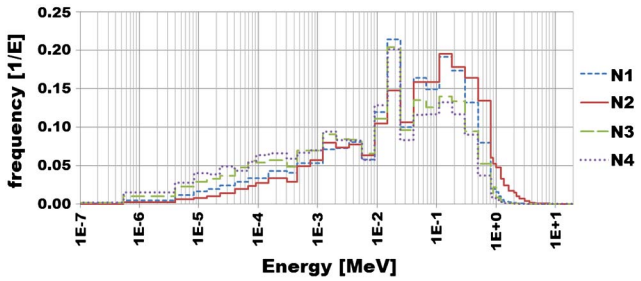

Fig. 4 Neutron flux spectra comparison of N1–N4 "nose plane" points. The averaged energy of the spectrum varies significantly due to scattering and absorber materials

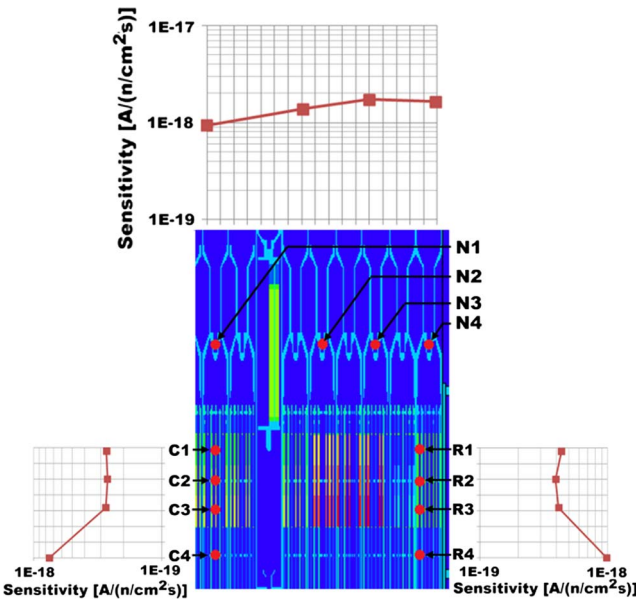

Fig. 5 Photonis CFUE32 FC current mode sensitivity in the positions studied in demonstrator ALFRED (uncertainty <1%)

maximum tolerable rate of free-in-air kerma stated by the manufacturer (~3 Gy/s [13,14]) makes the detector operable till 300 kW$_{th}$ and (2) gamma interferences in the current mode have to be evaluated very carefully because of the instrument sensitivity to gamma radiation. This issue is critical for installations near the fuel active zone because gamma interferences are negligible some meters away from the core, e.g., on nose plane points or outside the reactor vessel.

It is clear that typical miniaturized FCs (activated by ^{235}U) could be useful in monitoring the start-up and the lower section of the

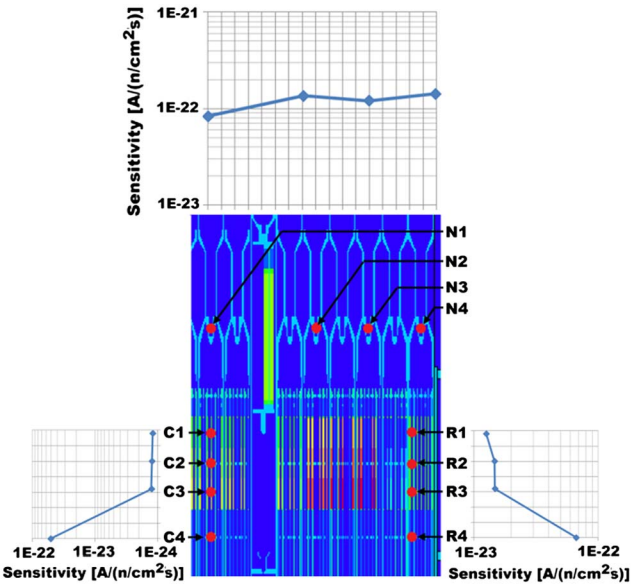

Fig. 6 KWD 5503-Co-210 SPND current mode sensitivity in the positions studied in demonstrator ALFRED (uncertainty <1%)

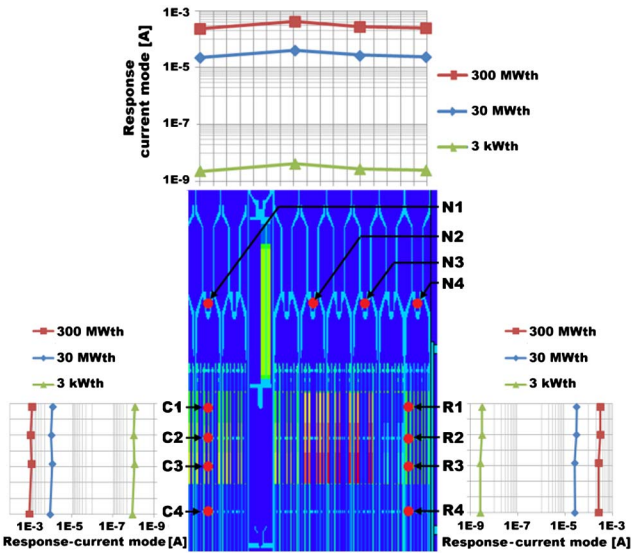

Fig. 7 Photonis CFUE32 FC current mode response in the positions studied in demonstrator ALFRED (uncertainty <5%)

intermediate range of reactor power (till 300 kW_{th} in ALFRED). When such a maximum power is reached, FCs must be driven away from the core and placed in rest positions or for monitoring new points far from the active zone, e.g., in the rear of the heat exchangers, using those objects as shielding.

About KWD SPND 5503-Co-210, in previous works [7], the author showed that the operation of those instruments requires a neutron population of some MW in magnitude to get neutron fluxes sufficient to produce reliable outcoming signals. Its sensitivity, some decades lower than Photonis CFUE32 FC, ensures the possibility of a fixed installation in the fuel element lattice, enabling the operation of detectors only when a certain minimum power is reached. The durability of this sensor is less critical than in uranium FCs, as the burnup rate is significantly lower, i.e., burnup at 1% per year at full power.

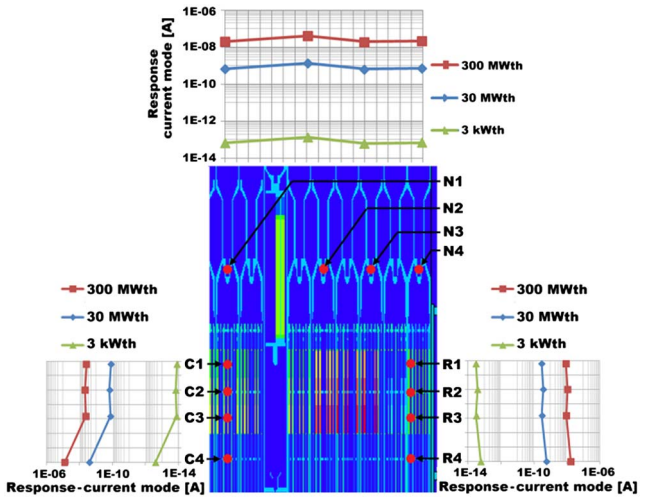

Fig. 8 KWD 5503-Co-210 SPND current mode response in the positions studied in demonstrator ALFRED (uncertainty <5%)

In this work, the gamma field was characterized throughout free-in-air kerma (doses are reported in Table 3) as a primary evaluation for analyzing the gamma contribution to the sensors' signals. This aspect is being studied and an extensive treatment will be included in the continuation of this work. Qualitatively, it can be stated that this issue is critical with the sensor installed into the core active zone, where gamma flux intensities and averaged energies find their maxima. Installation points into the reflector surrounding the core suffer this issue slightly. Points on the nose plane are protected from the gamma radiation interference due to the lead plenum above the active zone of the reactor core.

It must also be noted, however, that the studied instrument has very little quantity of sensitive material: a larger volume of emitter can be introduced into the sensor if more sensitivity is needed. It must be noted, however, that a detector's sensitivity is not proportional to the increase in sensitive material because geometrical considerations have to be taken into account.

At this stage of the work, prompt SPNDs seem to be very promising as in-core instrumentation for neutron-flux control purposes in the power range.

6 Proposal for New Detector Designs for Customized Application in LFR

This work shows that FCs are sensitive enough to follow the start-up and the intermediate range of the reactor power properly, keeping detector workability for some years or more. Variations of FC sensitivity cannot resolve the durability issue of these instruments, which in no way can be used for continuous monitoring of the power range in core proximity.

FCs can be optimized in design and operation for low/intermediate power monitoring, customizing sensitivity and signal-to-noise ratio decade per decade, by controlling some important parameters of the instrument. One of the main drawbacks is the increasing leakage current coming through the insulator material when the temperature rises; an artificial diamond can ensure better electrical resistivity in comparison with the commonly used alumina. Fissile consumption and fission product buildup are two detrimental effects that increase with neutron fluence of the instrument. The first effect can be compensated with a self-breeding FC, where burned fissile atoms can be replaced with fissile production by neutron capture on fertile material. Fission product buildup can only increase with fluence: a perspective could be the washing of the inert gas into the instrument by a venting channel to mitigate the negative effects

of the radioactive fission fragments. Moreover, a venting channel could be useful for changing the working gas pressure of the detector, optimizing this value according to the specific needs of the operated mode (pulse, MSV, or current modes).

Different possibilities are envisaged for a new layout of FCs, even if this customization may be not so necessary for instrumentation for full power monitoring.

SPNDs can be used successfully to overcome FCs drawbacks in full power monitoring: they are simple, sensitive enough to detect neutron fluxes in the power range, and robust enough to last a few years in reactor full power conditions. Therefore, prompt SPNDs can have a key role into LFR core neutron flux monitoring and control.

Usually, SPNDs are used for in-core monitoring purposes to retrieve neutron flux shape information both axially and radially, but such information is not relevant to reactor safety; therefore, delayed responses by the instruments are accepted (this is the field of application of rhodium and vanadium SPNDs, the most used). Prompt SPND like cobalt SPNDs are not so used and hence their evolution experiences a steady state.

Hereafter, new perspectives for cobalt SPNDs (or more generally prompt-SPNDs) are proposed to customize this kind of detector for the LFR environment. As shown above, the studied instrument succeeds in full power continuous monitoring, but stronger response by the instrument could be more reliable and easy to retrieve. This goal is reachable by adding sensitive material to the instrument because the electric signal strength depends on the number of capture reaction only; alternatively, some instruments can be electrically put in parallel for collecting currents greater in magnitude. An assembly design for SPNDs could be useful for driving activation probes, and calibrating periodically the detector. Moreover, the assembly design could behave better in reliability analysis because it is more difficult that all parallel detectors fail simultaneously.

SPNDs are originally nonradioactive because they become radioactive only when exposed to a neutron flux. It means that detector construction is pretty easy because no radioactive manipulation is needed, as with FCs, which do imply the manipulation of alpha emitters. This peculiarity makes SPNDs cheap and fast to be manufactured, allowing the installation of more sensors in a single batch and their substitution after irradiation not so expensive.

7 Conclusion and Future Developments

The simulations conducted in this study show that the LFR demonstrator, ALFRED, can be supplied with some kind of FCs and SPNDs currently available as in-core control instrumentation, but those detectors could be not completely suitable for this kind of reactor.

Improvements can be made in detector designs to customize sensitivities, as requested by neutron monitoring needs of the peculiar reactor.

FCs seem to be the best and unique solution for monitoring the reactor power at the lower decades of neutron flux, i.e., at start-up and intermediate range. Because of their removal when a certain power is reached (to preserve the integrity of the instruments), handling devices must be studied and included into the reactor design, maybe with some guide tubes dedicated for neutron detectors.

SPNDs seem to be the best compromise for monitoring the higher decades of neutron flux, i.e. when reactor is operated at power range. They can be installed in a fixed configuration and used only when the neutron population becomes sufficient to produce reliable signals. Gamma interferences must be evaluated carefully in positions inside the core active zone. Different materials, with lower sensitivity to the gamma radiation, can be evaluated.

Although FCs were experimented in SFR fast fluxes in the 1970s [15], prompt SPNDs seem to have no concrete irradiation experience in such an environment.

Due to the lack of R&D about prompt SPNDs, some significant improvements are envisaged: because of that, those detectors will be the focus of the future steps of this work. In order to optimize the SPND design by MCNPX, some experimental tests of commercial SPNDs carried out at the ENEA TAPIRO Fast Reactor facility [16] have been reconstructed into the Monte Carlo code. The successful reproduction of the experimental results validates the simulation model for those instruments, elevating MCNPX as a design tool. Future developments will include an extensive study on SPND modifications; new designs of custom-made prompt SPND could be prototyped and new tests scheduled.

Acknowledgment

The authors would like to express special thanks to Dr. Mario Carta, head of ENEA Casaccia FSN-FISS-RNR, and Dr. Lina Quintieri of ENEA Casaccia INMRI Institute for their precious advice and infinite disposability in dialogue. A special thanks goes to all ENEA\UTICT technicians, in particular to Eng. Guido Guarnieri, for their perseverance, disposability, and competency in solving all issues about HPC. The computing resources and the related technical support used for this work have been provided by CRESCO/ENEAGRID High Performance Computing infrastructure and the staff [17]. CRESCO/ENEAGRID High Performance Computing infrastructure is funded by ENEA, the Italian National Agency for New Technologies, Energy and Sustainable Economic Development, and by Italian and European Research Programmes; see http://www.cresco.enea.it/english for more information. This work was partially supported by the Research Contract PAR2014, ADPFISS – LP2 – 089, Italian Ministry for Economic Development and ENEA.

Nomenclature

C‘i’	= measurement point ‘i’ on core central axial traverse referring Fig. 2
cps	= count per second [s^{-1}]
E	= Energy [MeV]
ESCF($\rightarrow r$)	= local Energy Spectrum Correction Factor [-]
fast	= fast, referring to fast neutron
Gy	= Gray [J/kg], absorbed dose or kerma unit measurement
$h \times core$	= computational power [hour·core]
n	= neutrons
nv	= neutron flux, equivalent to $p(\rightarrow r)$
N‘i’	= measurement point ‘i’ on nose plane radial traverse referring Fig. 2
$p(\rightarrow r)$	= neutron flux magnitude factor [n/($cm^2 \cdot s$)]
$\rightarrow r$	= vector for position
$R(\rightarrow r)$	= local detector response [A^2/Hz] or [A]
R‘i’	= measurement point ‘i’ on reflector axial traverse referring Fig. 2
$S(\rightarrow r)$	= local detector sensitivity [A^2/(Hz · nv)] or [A/nv]
T	= temperature [°C] or [K]
th	= thermal, referring to thermal power
thermal	= thermal, referring to thermal neutron
y	= year
$\varphi(E, \rightarrow r)$	= local neutron flux per unit energy [n/($cm^2 \cdot s \cdot E$)]
$\psi(E)$	= neutron flux energy spectrum shape factor [1/E]
$\sigma_i(E)$	= microscopic cross-section of reaction i used by detector [barn]
$\bar{\sigma}_i(\rightarrow r)$	= energy-averaged local cross-section of reaction i used by detector [barn]

References

[1] Generation IV International Forum, 2002, “A Technology Roadmap for Generation IV Nuclear Energy Systems,” GIF-002-00.

[2] Salvatores, M., and Palmiotti, G., 2011, “Radioactive Waste Partitioning and Transmutation within Advanced Fuel Cycles: Achievements and Challenges,” Prog. Particle Nucl. Phys, **66**(1), pp. 144–166.

[3] Lepore, L., Remetti, R., and Cappelli, M., 2013, "Analisi Dei Sistemi di Strumentazione e Controllo Previsti in Alcuni Progetti su Reattori al Piombo Attualmente in Sviluppo a Livello Internazionale," ENEA-MSE Report RdS/2013/030, http://www.enea.it/it/Ricerca_sviluppo/documenti/ricerca-di-sistema-elettrico/nucleare-iv-gen/2012/rds-2013-030.pdf.
[4] SCK-CEN, 2016, "MYRRHA: An Accelerator Driven System (ADS)," *SCK-CEN*, http://myrrha.sckcen.be/en/MYRRHA/ADS.
[5] Alemberti, A., 2012, "The European Lead Fast Reactor Design, Safety Approach and Safety Characteristics," ELFR, Dresden, https://www.iaea.org/NuclearPower/Downloadable/Meetings/2012/2012-03-19-03-23-TM-NPTD/14_TM-Safety-Dresden_Italy_Alemberti.pdf.
[6] Lepore, L., Remetti, R., and Cappelli, M., 2014, "Fast Neutron-Flux Monitoring Instrumentation for Lead Fast Reactors: A Preliminary Study on Fission Chamber Performances," 22nd International Conference on Nuclear Engineering Proceedings (ICONE22), V006T13A016, ASME, Prague, 9.
[7] Lepore, L., Remetti, R., and Cappelli, M., 2015, "Evaluation of the Current Fast Neutron Flux Monitoring Instrumentation Applied to LFR Demonstrator ALFRED: Capabilities and Limitations," 23rd International Conference on Nuclear Engineering Proceedings (ICONE23), Makuhari Messe, Chiba, Japan, JSME.
[8] Briesmeister, J. F., 2016, "MCNP–A General Purpose Monte Crlo Code for Neutron and Photon Transport," www.iaea.org/inis/collection/NCLCollectionStore/_Public/18/044/18044302.pdf.
[9] Alemberti, A., 2013, "The Lead Fast Reactor: Demonstrator ALFRED and ELFR Design," Paris, https://www.iaea.org/nuclearenergy/nuclearpower/Downloadable/Meetings/2013/2013-03-04-03-07-CF-NPTD/T2.1/T2.1.alemberti.pdf.
[10] Gauthier, J. C., Granget, G., and Martini, M., 1989, "Techniques de Mesures Neutroniques au Demarrage de SPX2," Proceedings of a Specialists' Meeting on in Core Instrumentation and Reactor Assessment, CEA, Cadarache.
[11] Perrigueur, J. C., Berlin, C., Gauthier, J. C., and Gourdon, J., 1989, "In Core Neutronic Measurements in an Industrial Environment. Assessment of the Performances of the In-Vessel Neutronic Measurements Chains of SUPER-PHENIX 1," Proceedings of the Specialists' Meeting on in Core Instrumentation and Reactor Assessment, CEA.
[12] Nervi, J. C., Marmonier, P., Eyraud, A., Perrigueur, J. C., Rouches, P., and Verset, L., 1987, "Experimental Devices Used for Start-Up Operations of the SUPER-PHENIX Core," International Conference, ANS/ENS, Richland.
[13] Photonis, 2015, "Photonis Fission Chamber for In-Core Use," https://www.photonis.com/en/product/fission-chambers-core-use.
[14] Photonis, 2015, "Photonis Fission Chamber for Out-of-Core Use," https://www.photonis.com/en/product/fission-chambers-out-core-use.
[15] Trapp, J. P., Haan, S., Martin, L., Perrin, J. L., and Tixier, M., 1997, "High Temperature Fission Chambers: State-of-the-Art," In-Core Instrumentation and Reactor Core Assessment. Proceedings of a Specialist Meeting, NEA, Mito-shi, Japan.
[16] Angelone, M., Klix, A., Pillon, M., Batistoni, P., Fischer, U., and Santagata, A., 2014, "Development of Self-Powered Neutron Detectors for Neutron Fluxmonitoring in HCLL and HCPB ITER-TBM," Fusion Eng. Des., **89**, p. 2194–2198.
[17] Ponti, G., 2014, "The role of medium size facilities in the HPC ecosystem: the case of the new CRESCO4 cluster integrated in the ENEAGRID infrastructure," International Conference on High Performance Computing and Simulation, IEEE.
[18] ARi Industries, 2015, "Self Powered Neutron Detectors," http://www.ariindustries.biz/wp-content/uploads/2015/02/019_self_powered_neutron_detectors.pdf.
[19] KWD Nuclear Instruments, 2016, "Self Powered Neutron Detectors," http://www.kwdnuclearinstruments.se/self-powered-neutron-detectors.